V-H-M Seismic Capacity Envelopes of Strip Foundations on Slopes for Capacity Design of Structure-Foundation System

Dhiraj Raj[1], Yogendra Singh[2] and Amir M. Kaynia[3,4]

[1]*Research Scholar, Department of Earthquake Engineering, Indian Institute Technology Roorkee, Roorkee 247-667, India, E-mail: dhirajraj.iitr@gmail.com*

[2]*Professor and Head, Department of Earthquake Engineering, Indian Institute Technology Roorkee, Roorkee 247-667, India (corresponding author), E-mail: yogendra.eq@gmail.com*

[3]*Professor, Department of Structural Engineering, NTNU, NO-7491 Trondheim, Norway. E-mail: amir.kaynia@ntnu.no*

[4]*Technical Expert, Norwegian Geotechnical Institute, P.O. Box 3930 Ullevaal Stadion, 0806 Oslo, Norway, E-mail: amir.m.kaynia@ngi.no*

Abstract: The columns and the supporting foundations are invariably subjected to the interacting axial force, *V*, shear force, *H* and moment *M*. It is quite common to consider the interaction of these forces in design of structural components, but the available standards and literature usually ignore the effect of interaction in case of foundations on slopes. Further, very little information is available about seismic capacity of foundations located on slopes. This article presents a numerical study on evaluation of the *V-H-M* capacity envelopes of strip foundations placed on top and face of slopes and subjected to earthquake action, with an objective of enabling a direct comparison with the capacity of the supported columns. Nonlinear 2D finite element limit analyses (FELA) are performed for this purpose. Modified 'Probe' analyses are carried out for two representative c-ϕ soil slopes to develop the *V-H-M* capacity envelopes. The computed capacity envelopes are compared with their counterparts on flat ground. The characteristic features of the capacity envelopes are identified and explained considering the failure patterns under different combinations of *V*, *H* and *M*. A comparison of the capacity envelopes of counterpart foundations on flat ground and of columns is presented to highlight the relative hierarchy of strength of columns and foundations of a typical building on slope.

Keywords: Capacity envelope; Slope-foundation interaction; Seismic loading; Finite element limit analysis (FELA); Capacity design

Introduction

In practice, foundations are invariably subjected to a complex interactive action of vertical force, *V*, horizontal shear force, *H*, and moment, *M*. However, the majority of standards and codes of practice (IS6403 2002; EN1997-1 2004), while estimating the bearing capacity of shallow foundations, consider the effect of *H* and *M* using different correction factors. These correction factors have been developed separately for *H* and *M*, without considering the interaction between the three load components.

Some of the standards/codes (e.g. (EN1998-5 2004; NCHRP 2010; ASCE/SEI41-17 2017)) do provide empirically/analytically derived *V-H-M* capacity (or failure) envelopes (Lesny 2006; Lesny 2009) to check the safety of shallow foundations. Apart from these standards, some literature is also available on estimation of interactive failure loads for shallow foundations placed on flat ground consisting of cohesive (Ukritchon et al. 1998; Taiebat and Carter 2000; Gourvenec and Randolph 2003; Yun and Bransby 2007; Gourvenec 2007a; Gourvenec 2007b; Gourvenec 2008; Taiebat and Carter 2010; Vulpe et al. 2014; Shen et al. 2016) or cohesionless soils (Gottardi et al. 1999; Loukidis et al. 2008; Tang et al. 2015). A few experimental studies have also been reported in literature on shallow foundations subjected to *V-H-M* loading (Nova and Montrasioa 1991; Gottardi and Butterfield 1993; Butterfield and Gottardi 1994; Gottardi and Butterfield 1995; Montrasioa and Nova 1997; Martin and Houlsby 2000; Govoni et al. 2010; Cocjin and Kusakabe 2013). However, all of the available studies deal with shallow foundations on flat ground, and consider either cohesive or cohesionless soils. Moreover, most of them do not include the seismic conditions.

A few studies (Georgiadis 2010; Baazouzi et al. 2016) have considered only *V-H* interaction of shallow foundations located on top of slopes. Georgiadis (2010) performed a parametric study using finite element, upper bound plasticity, and stress field methods, on foundations located on top of slopes consisting of cohesive soil, and proposed empirical

equation for *V-H* capacity envelope. Baazouzi et al. (2016) conducted a study on *V-H* load interaction in shallow foundations placed on top of a slope consisting of cohesionless soil, and found that the shape of the interaction diagram depends on the slope angle and the distance of the foundation from the slope. No studies could be found in the literature on capacity envelopes of foundations located on slope face with or without the effect of seismic action.

In this article, the *V-H-M* capacity envelopes for strip foundations placed on homogenous *c-ϕ* soil slopes are evaluated. The slope mass is subjected to seismic action represented by horizontal seismic coefficient, α_h, in addition to the loads from the superstructure which include the seismic structural loads. The slope mass has been subjected to a constant body force proportional to α_h, whereas the force from the superstructure has been gradually increased till incipient failure of the foundation-slope system. Finite element limit analyses (FELA) were conducted using the proprietary software OptumG2 (2018). A comparison of the *V-H-M* capacity envelopes on slopes is presented with the corresponding envelopes for the foundations placed on flat ground. In addition, the relative hierarchy of capacity of foundations and the counterpart columns of a typical reinforced concrete (RC) frame building on slope, designed according to the relevant standards and literature, has been explored to examine the validity of the failure patterns assumed in conventional design.

V-H-M Interaction on Slopes

Figure 1 illustrates the generalized planar actions on a pier of a typical bridge and on the columns of a building. It can be seen from the figure that the moment and shear force in the pier/columns are not independent quantities, rather related through the effective height *h* (that is, $M = h \times H$), which is equal to the total height in case of a cantilever pier, and equal to the height of the point of contra-flexure from foundation in case of the columns of the building frame.

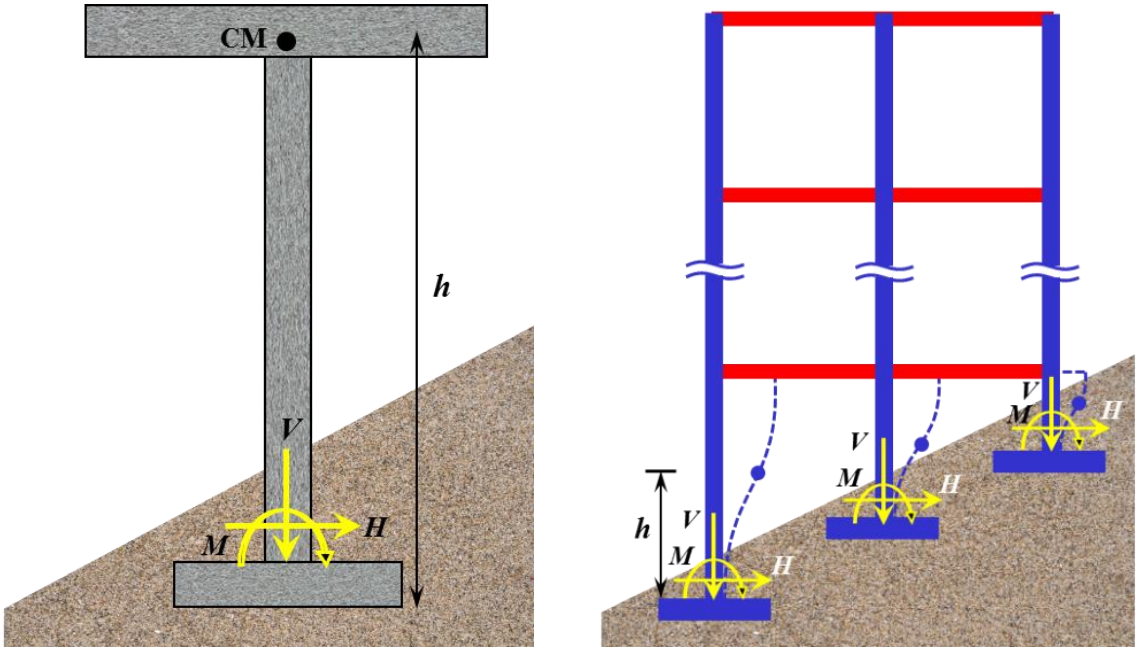

(a) (b)

Fig. 1. Effective height of typical structures on slope: (a) A single pier bridge; and (b) Moment resisting frame building

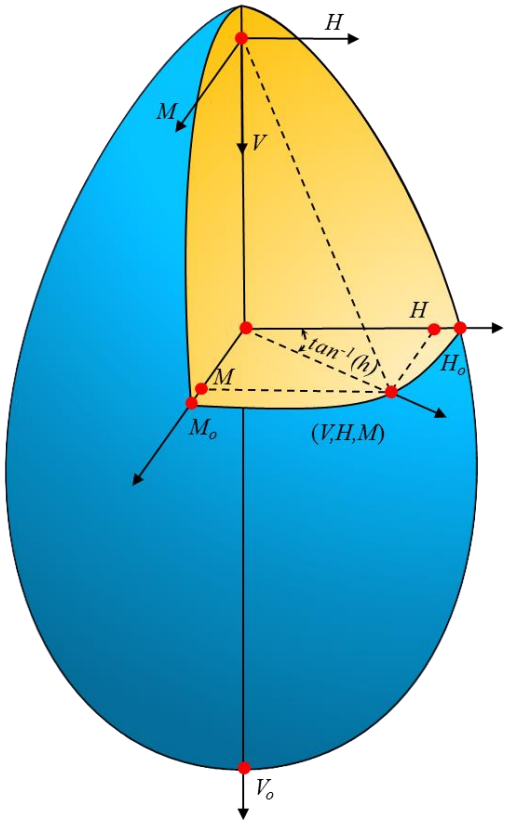

Fig. 2. Intercative *V-H-M* forces and schemetic of capacity enevelope of a typical foundation (H_o and M_o are the horizontal shear and moment capacity, respectively, at a given vertical load, *V*, without considering the *H-M* interaction)

Figure 2 illustrates the interaction of V, H and M actions and schematic of the capacity envelop for a typical foundation. At a given value of V, the interactive capacity (H and M) is lower than the independently obtained capacity (H_0 and M_0). Further, as explained earlier, for a given cantilever column, the H-M pair follows a radial path in the H-M plane, along the line $M/H = h$. In case of a multi-column frame also, the effective height, h is constant (resulting in a radial path of H-M pair) till the onset of yielding, but varies after that. This inter-relation underlines the dependence of the interactive V-H-M capacity of a foundation on the type and configuration of the supported structure. This is particularly important in case of hill-side buildings (buildings located on face of slopes), which have foundations constructed at different levels resulting in columns of different heights with dramatic effect on the corresponding foundation capacity.

Problem Statement

In this study, the capacity envelope of strip foundations placed at different locations on a slope has been estimated by performing a series of finite element limit analyses. Two homogeneous slopes, one representing a stiff clay and the other a dense sand, have been considered in this study with material properties as shown in Table 1 (Fotopoulou and Pitilakis 2013). Both slopes have a height of 40 m, but have different inclination angles, $\beta = 20°$ and 30° from horizontal. The large inclination angles have been selected to clearly highlight the impact of sloping ground on capacity envelope. Finite element limit analysis (FELA) based on strength reduction technique has been used to estimate the static factor of safety (FOS) of the slopes. The FOS was computed equal to 2.3 and 2.0, for the 20° (stiff clay) and 30° (dense sand) slopes, respectively. Pseudo-static approach has been used to obtain the FOS under seismic loading. Coincidently, both slopes become unstable at a horizontal seismic coefficient, $\alpha_h = 0.36g$ (g is acceleration due to gravity). In this study, a rigid rough strip foundation with width, $B = 2$ m

and zero offset distance from slope edge located on top and face of the slopes has been considered as shown in Fig. 2. The figure also shows the general planar (*V*, *H* and *M*) loading acting on the foundation and seismic action (α_h) acting on the soil. The effect of seismic action on the superstructure is included in the general planar loading (*V*, *H* and *M*). The sign convention for applied loads and moment following inside right hand rule (Butterfield et al. 1997), is also shown in Fig. 3. The strip foundation located on top of the slope is placed on the ground surface, i.e. without any embedment, whereas the strip foundations located on the slope face have varying depth of embedment in the soil mass as shown in Fig. 3. For the purpose of comparison, the same foundation is also considered on flat ground with identical soil properties.

Table 1. Material properties (Fotopoulou and Pitilakis 2013)

Properties	Soil Type	
	Stiff Clay	Dense Sand
Unit Weight, γ (kN/m^3)	20	20
Poisson's Ratio, v	0.3	0.3
Cohesion, c (kPa)	50	10
Angle of internal friction, ϕ	27°	44°

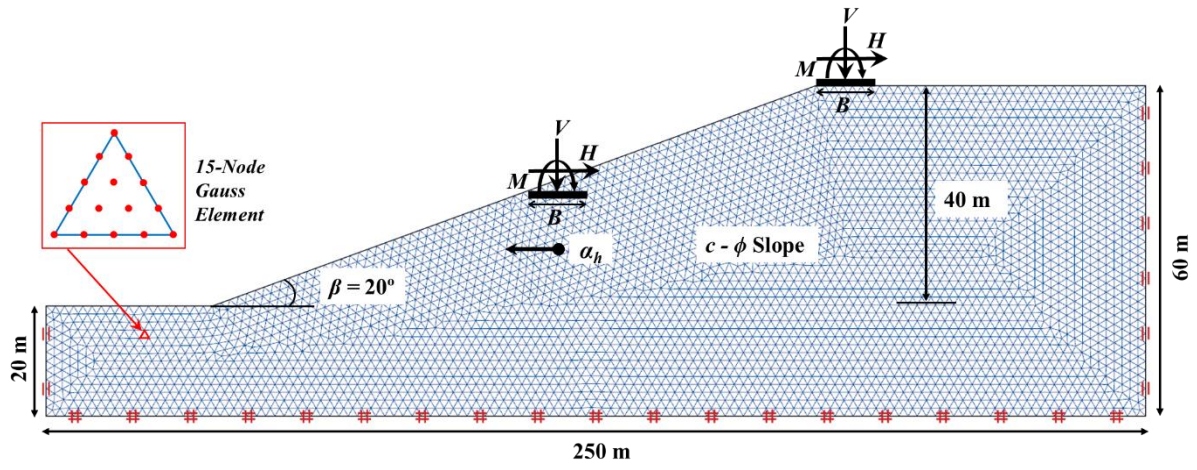

Fig. 3. Typical Finite element model (in OptumG2 (2018)) showing strip foundation located differently (on the top and on the face) on slope, under general planar loading

The relative hierarchy of strength of the superstructure and foundation is important in the context of capacity design philosophy of the modern seismic design codes (EN1998-5 2004; IS1893 2016; ASCE/SEI41-17 2017). To examine the relative capacity, the interactive capacity of typical columns of a generic two storey RC frame building, having irregular 'step-back' configuration, located on face of the stiff clay slope has been compared with the capacity envelopes of the supporting strip foundations, designed according to various standards and literature.

Modelling features

Application of plastic bound theorems of limit analysis in geotechnical stability problems is widely known and has been extensively discussed by others (see for example Chen and Liu (1990)). Combination of limit analysis with finite element discretization enhances the capabilities of both numerical methods and enables the combined method, FELA, to bracket the exact limit load by the upper-bound (UB) and lower-bound (LB) solutions for handling complex problems in geotechnical engineering with irregular geometries, varying soil properties, loadings, and boundary conditions (Sloan 2013; Raj et al. 2018a). The analyses presented in this paper have been performed using OptumG2 (2018) software, in which both UB and LB problems under plane-strain condition are formulated using the so-called second-order cone programming (SOCP) (Makrodimopoulos and Martin 2006; Makrodimopoulos and Martin 2007). In addition to LB and UB limit analysis, this numerical tool provides the option of 15-node triangular mixed element (Fig. 3) from Gauss family for FELA. The details of numerical formulation of FELA can be found in Krabbenhoft et al. (2016).

To develop the capacity envelope in *V-H-M* space, and to identify the different failure mechanisms, 2D plane-strain nonlinear Finite Element (FE) models of the slopes with strip foundation have been developed. An elasto-plastic constitutive model based on Mohr-Coulomb

failure criterion and following associated flow rule has been used for modeling of soil in FELA. It will be shown in the next section that the assumption of associated flow rule, does not have a significant effect on the results of interest in the present study. The soil mass has been discretized using plane strain triangular elements with 15-node mixed Gauss element formulation (Fig. 3). The foundation has been modelled using two-noded elastic 'plate' element, which acts like the standard Euler-Bernoulli beam element in plane-strain domain. A rigid elastic material (approximated using relatively large value of Young's modulus) has been considered for the foundation. The soil-foundation interaction has been considered by assigning interface elements (with velocity and stress discontinuities) on one side (in case of surface foundation) or on both sides (in case of embedded foundation) of the foundation. The same material properties as for the surrounding soil (i.e. interface strength reduction factor, R = 1), but with zero tension cut-off, have been assigned to the interface element to simulate rough foundation with gap and uplift.

The base of the FE model has been fixed in both translational directions, whereas only horizontal movement has been restrained on the left and right lateral boundaries. Using a sensitivity study, the lateral extent and depth of the FE model have been selected in such a way that the effect of boundary conditions and model dimensions on the domain of interest is insignificant. To bracket the limit load as close as possible to the exact load, adaptive meshing with four iterations has been used in all the analyses. For each analysis, the number of elements has been varied from 8000 to 10,000.

Numerous combinations of V, H and M have been used in a series of FELA to evaluate the capacity envelope in V-H-M space. The modified form of the so-called 'constant force-ratio probe' (Taiebat and Carter 2000) methodology (see Fig. 4) has been adopted to develop full V-H-M capacity envelope. To this end, the foundation-slope system was analysed for 32 different fixed ratios of horizontal force, H, and moment, M, representing different effective height, h of

superstructure (as illustrated in Fig. 1) at any given value of the vertical load, *V*. The different values of the vertical load, *V* were selected as fraction multiples (1/6, 1/3, 1/2, 2/3, 5/6, 1.0, 1.1, 1.2, 1.3, 1.5 and 2.0) of the maximum capacity of the foundation under pure vertical loading. The reason for this selection is that, as it is shown later in this paper, in case of foundations on slopes, the vertical load capacity can in some cases exceed the maximum vertical load capacity without shear and moment.

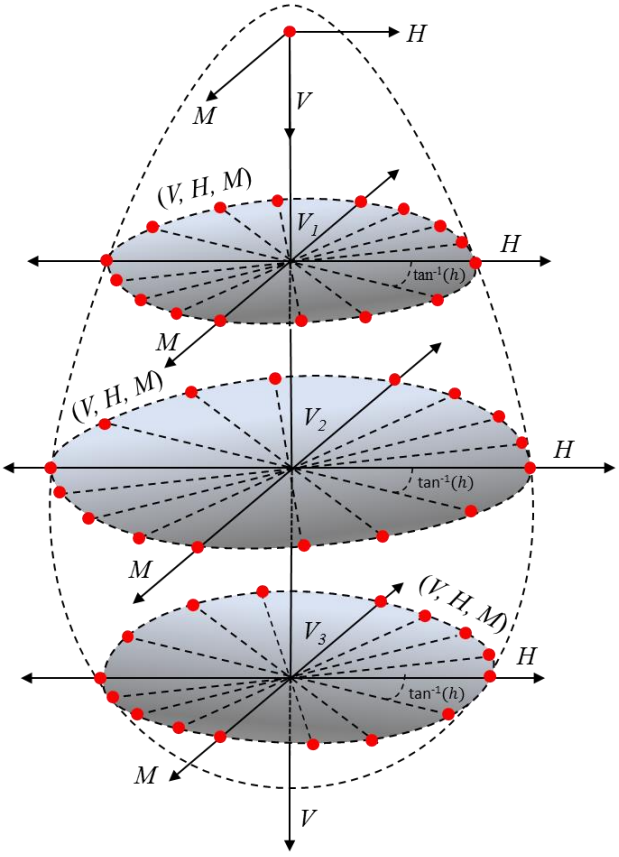

Fig. 4. Schematic diagram illustrating the procedure used to develop the *V-H-M* capacity envelope

Some of the past researchers (Bransby and Randolph 1998; Gottardi et al. 1999; Gourvenec and Randolph 2003; Gourvenec 2007a) have used a displacement based methodology or swipe technique to develop the capacity envelopes. Figure 5 (a-b) compares the normalized load-displacement curves for horizontal shear and moment obtained using

swipe technique with the normalized capacities estimateded using FELA. The vertical load, horizontal load, and moment, have been normalized as:

$$\bar{\mathrm{V}} = V_{\beta,\alpha_h} / V_0 \tag{4}$$

$$\bar{\mathrm{H}} = H_{\beta,\alpha_h} / V_0 \tag{5}$$

$$\bar{\mathrm{M}} = M_{\beta,\alpha_h} / BV_0 \tag{6}$$

where, $\bar{\mathrm{V}}$, $\bar{\mathrm{H}}$, and $\bar{\mathrm{M}}$ are the normalized vertical load, horizontal load, and moment, respectively, V_{β,α_h}, H_{β,α_h} and M_{β,α_h} are the vertical load, horizontal load and moment for the strip foundation placed on the slope with inclination angle, β and subjected to seismic coefficient, α_h; and V_0 is the pure vertical load capacity (i.e. for $H = M = 0$) of the strip foundation placed on flat ground.

As mentioned earlier, in case of FELA an associated flow rule has been assumed, whereas in case of swipe analysis, a non-associated flow rule (with $\psi = 14°$) has been assumed. Further, as FELA provides only the final estimate of the capacity, and not the load-displacement curve, the obtained capacities have been shown by horizontal straight lines. The curves have been shown for a typical foundation (with $B = 2$ m) located on top of the dense sand slope, subjected to a vertical load equal to $V_{max}/3$ (V_{max} is the maximum vertical load capacity at $H = M = 0$, for the given slope and seismic coefficient) and $\alpha_h = 0.20$ g. Similarly, Fig. 5(c) compares the *H-M* capacity points, of the same foundation subjected to the same α_h, obtained using the probe (FELA) and swipe (displacement controlled) methods. The different curves (A - F) in Fig. 5(a-b) represents different combinations of *H* and *M*, marked in Fig. 5(c) on the normalized *H-M* envelope.

Although, there is about 20-40% increase in the estimated capacity in case of associated flow rule assumption, it can be observed from the figure that both the methods lead to identical

normalized capacity indicating that the flow rule does not have any significant effect on the normalized capacity envelope, as demonstrated earlier by Loukidis et al. (2008).

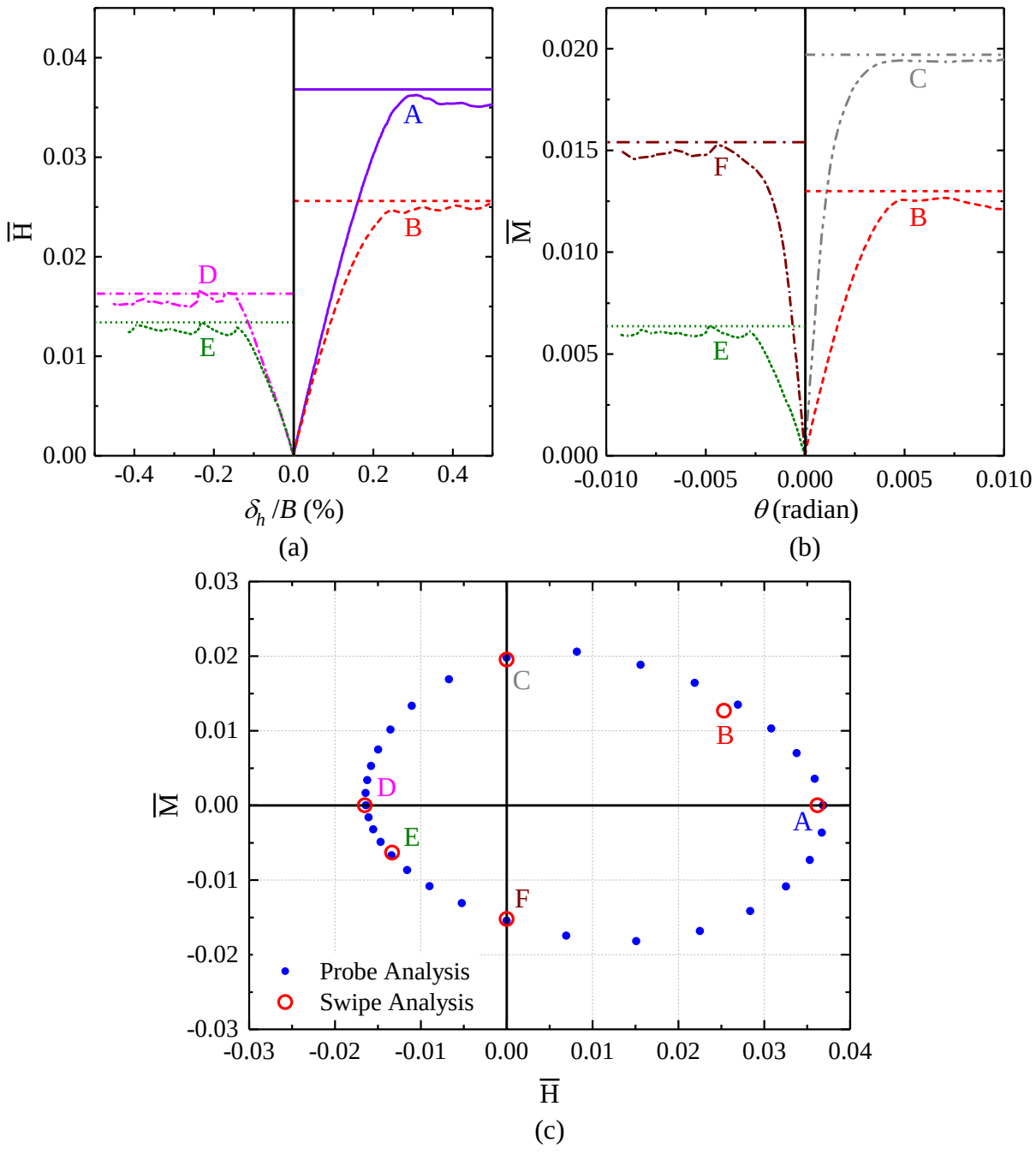

Fig. 5. A comparison of the normalized *H-M* capacity at $V_{max}/3$, obtained using displacement based (swipe) method considering non-associated flow rule and constant force ratio (probe) method using FELA considering associated flow rule: (a) variation of normalized shear ($\overline{H}$) with normalized horizontal displacement (δ_h/B); (b) variation of normalized shear ($\overline{M}$) with rotation (θ); and (c) capacity points in *H-M* plane. (In (a) and (b) the curves show the results of the swipe analysis, whereas the horizontal straight lines denote the probe analysis).

Model Validation and Comparison with Past Studies

To validate the considered plane-strain FE model, normalized static *V-H-M* capacity envelopes load have been compared for rigid rough strip foundation placed on surface of flat cohesionless ground (ϕ = 38° and γ = 20 kN/m^3) with those obtained from available standards (EN1998-5 2004; NCHRP 2010) and past studies (Butterfield and Gottardi 1994; Loukidis et al. 2008; Tang et al. 2015). Figure 6 presents a comparison of the *V-H-M* capacity envelope in *V-H*, *V-M* and *H-M* planes. The *H-M* envelopes have been shown for three different values of the normalized vertical load $\bar{V}$ (= 0.25, 0.50 and 0.75). It is evident from the figure that the present study predicts the capacity envelopes quite close to the most of considered standards/past studies, except in case of Butterfield and Gottardi (1994), which overestimates the capacity for cohesionless soil in *H-M* plane at higher vertical load ($\bar{V}$ = 0.50 and 0.75) up to 30%. Further, it is to be noted that the present study and Tang et al. (2015) have used FELA which is based on the assumption of associated flow rule. As illustrated in the previous section, the flow rule assumption does not have significant influence on the normalized capacity envelope.

To highlight the effect of slope inclination on the seismic capacity envelope, results of the present study for a rough foundation located on slopes of different inclinations (β = 0°, 10°, 20° and 30°) and subjected to α_h = 0.10 g, have also been compared (Fig. 7) with that of EN1998-5 (2004). It is to be noted that the EN1998-5 (2004) considers the effect of earthquake action, but does not provide capacity envelopes for foundations on slopes. The slopes have been assumed to be consisting of the same cohesionless soil as in case of flat ground. The comparison in Fig. 7 shows that the capacity envelopes obtained in the present study and EN1998-5 (2004) are quite close for β = 0°, under seismic action as well. However, the capacity reduces drastically with increase in slope inclination, making the use of EN1998-5 (2004) unsafe in case of foundations on slopes. This observation highlights the limitations of the available models in case of sloping ground, and need of the present study.

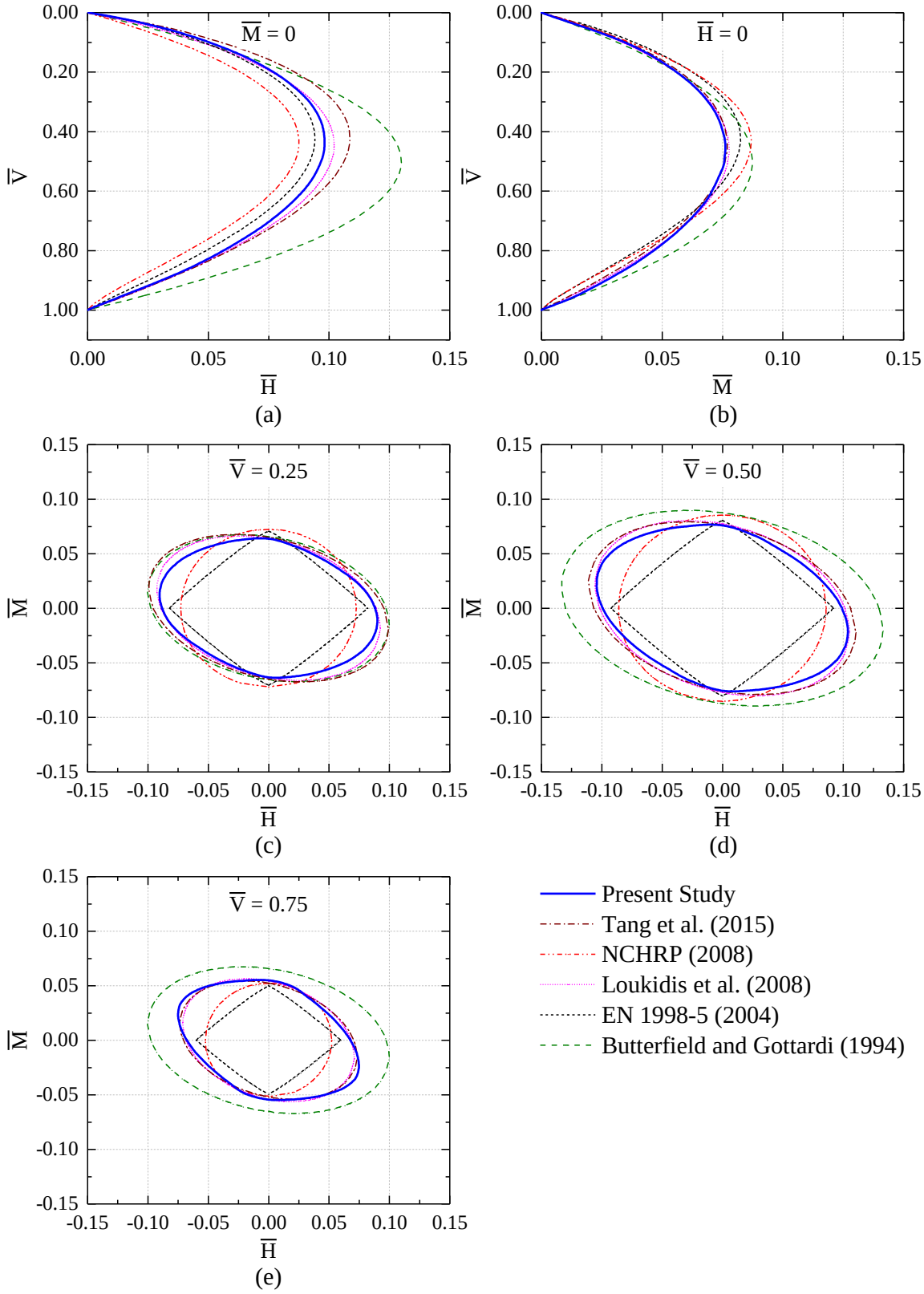

Fig. 6. Comparison of normalized *V-H-M* capacity envelopes for rigid rough strip foundation placed on surface of flat cohesionless ground: (a) normalized *V-H* envelope; (b) normalized *V-M* envelope; (c) normalized *H-M* envelope at normalized vertical load $\bar{V} = 0.25$; (d) normalized *H-M* envelope at normalized vertical load $\bar{V} = 0.50$; and (e) normalized *H-M* envelope at normalized vertical load $\bar{V} = 0.75$.

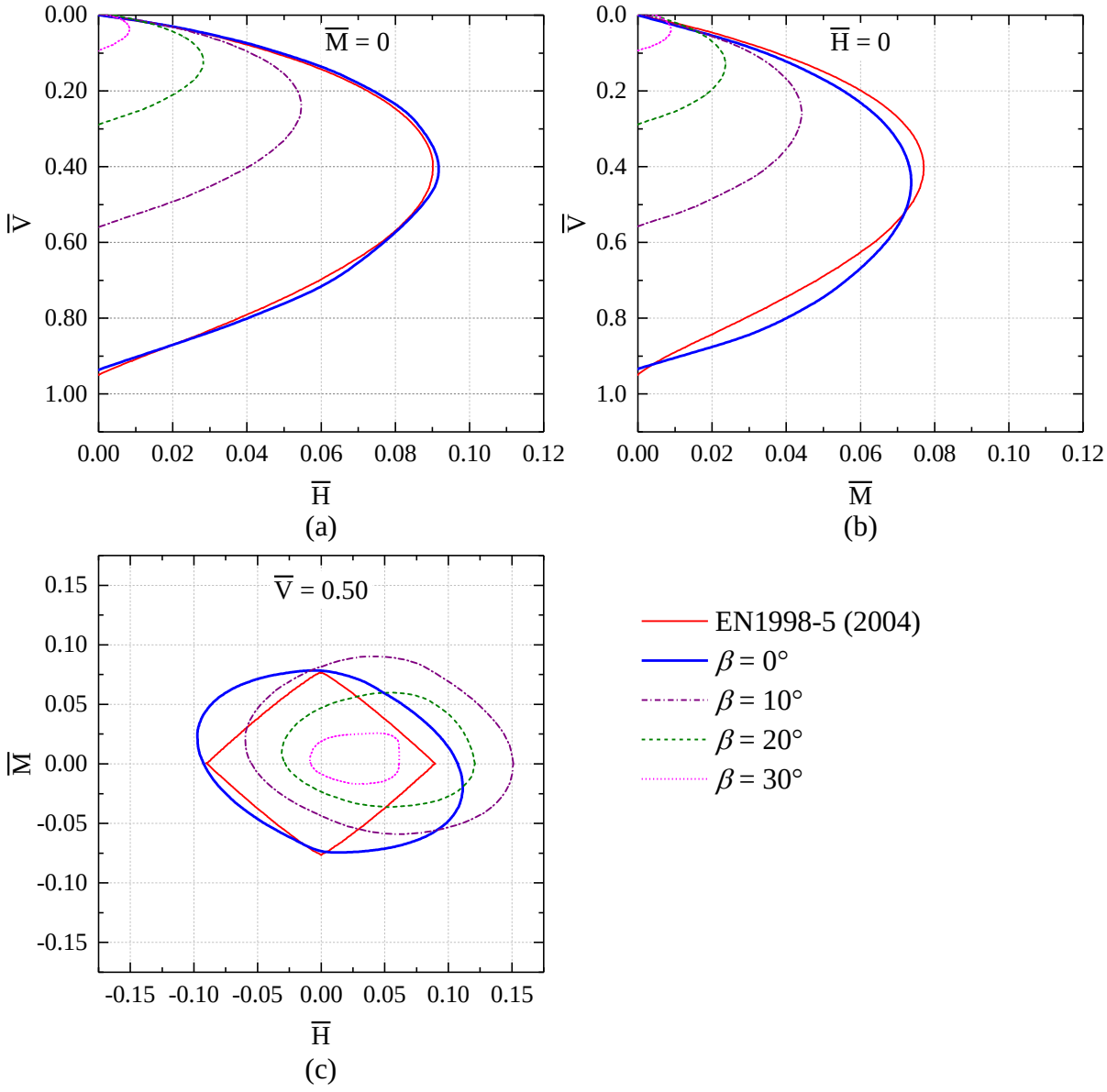

Fig. 7. Effect of slope inclination on normalized *V-H-M* capacity envelopes for rigid rough strip foundation placed on the face of cohesionless soil slopes, and subjected to α_h = 0.1 g: (a) normalized *V-H* envelope; (b) normalized *V-M* envelope; and (c) normalized *H-M* envelope at normalized vertical load $\bar{V}$ = 0.50. (Note: EN1998-5 (2004) capacity envelopes are available on flat ground, i.e. β = 0˚).

Results and Discussion

The three-dimensional capacity envelope provides a convenient way to examine the safety of a foundation subjected to any combination of forces and moments and also enables assessment of the consequences of any change in the loading direction (Taiebat and Carter 2000). In the following sections, influences of the governing parameters, such as α_h, β and foundation

location, on the *V-H-M* capacity envelope have been explored in detail. Failure patterns of the slope-foundation system under different combinations of *V-H-M* are also presented.

V-H-M seismic capacity envelope

Figures 8 and 9 show the normalised *V-H-M* capacity envelopes for strip foundations placed on top and face of the stiff clay and dense sand slopes and on the flat surface of the coorresponding ground. The values of V_0, used to obtained the normalised vertical load, $\bar{V}$, horizontal load, $\bar{H}$ and moment, $\bar{M}$, are 3070 kN/m and 11600 kN/m for stiff clay and dense sand, respectively.

Figures 8(a) and (b) show the normalised seismic *V-H-M* capacity envelopes for strip foundations placed on flat ground of stiff clay material, subjected to α_h = 0 and 0.2g, respectively. Similarly, Figures 8(c) and (d) present the normalised capacity envelopes at the top of the stiff clay slope, whereas Figures 8(e) and (f) show the capacity curves on the face of the stiff clay slope. The corresponding envelopes for the dense sand flat ground and dense sand slope are shown in Figure 9. It can observed from the figures that the shape of the *V-H-M* capacity envelope for the foundation on slope is highly asymmetric campared to the foundation on flat ground. This asymmetry of the capacity envelope increases with the slope angle and seismic coefficient. Here, the *V-H-M* capacity envelope of foundation placed on the face of the slope is larger than the one when the foundation is placed on top of the slope. This slight increase in the capacity of the foundation is due to partial embedment of the foundation. The increased capacity is primarily under positive direction of *H* and *M*; that is, horizontal force and moment acting towards the slope. However, this direction of loading is not critical in design of foundation and therefore does not have much practical significance.

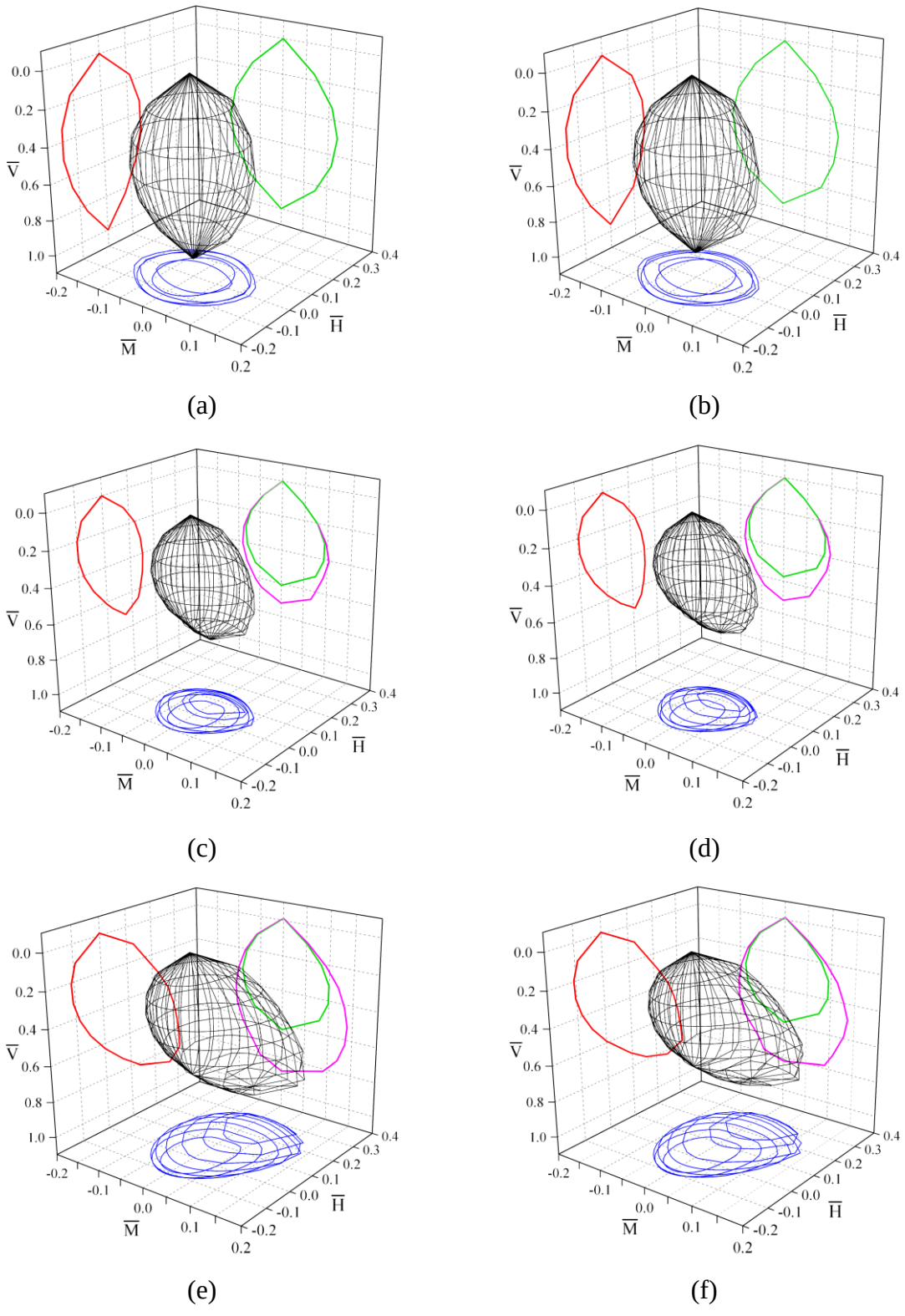

Fig. 8. *V-H-M* capacity envelopes and their projections in different planes (maximum envelope in V-H plane, maximum envelope and envelope at H = 0 in V-M plane, and *H-M* envelopes at different *V*), for stiff clay and: (a) foundation located at surface of flat ground with α_h = 0g; (b) foundation located at surface of flat ground with α_h = 0.2g; (c) foundation located on top of the 20° slope with α_h = 0g; (d) foundation located on top of the 20° slope with α_h = 0.2g; (e) foundation located on face of the 20° slope with α_h = 0g; and (f) foundation located on face of the 20° slope with α_h = 0.2g.

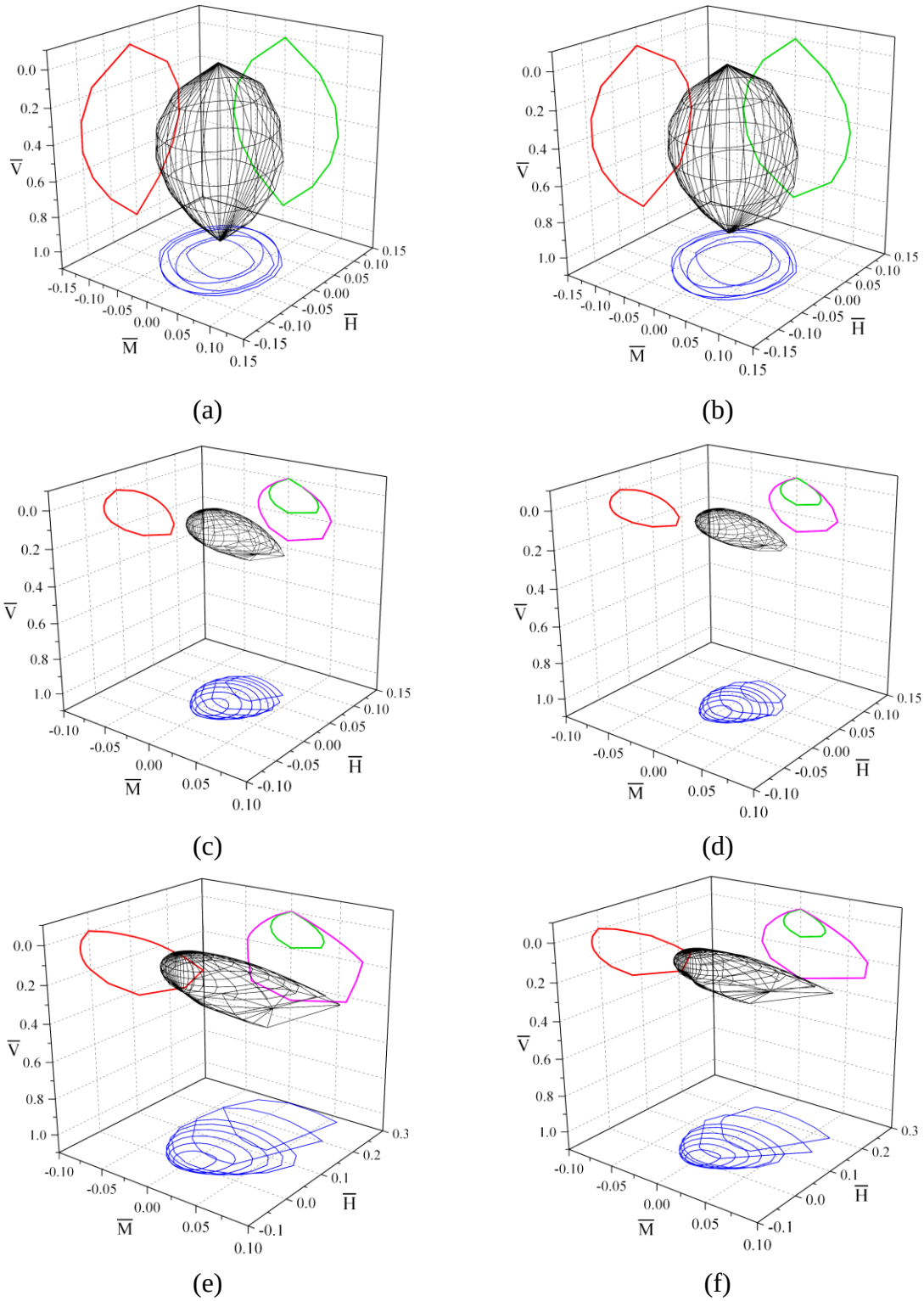

Fig. 9. *V-H-M* capacity envelopes and their projections in different planes (maximum envelope in V-H plane, maximum envelope and envelope at H = 0 in V-M plane, and *H-M* envelopes at different *V*), for dense sand and: (a) foundation located at surface of flat ground with α_h = 0g; (b) foundation located at surface of flat ground with α_h = 0.2g; (c) foundation located on top of the 30° slope with α_h = 0g; (d) foundation located on top of the 30° slope with α_h = 0.2g; (e) foundation located on face of the 20° slope with α_h = 0g; and (f) foundation located on face of the 20° slope with α_h = 0.2g. (Note that, due to large difference in the horizontal shear capacity of foundations located on top and face of 30° slope, the scale for $\overline{H}$ could not be kept uniform.)

The figures also show the projections of the *V-H-M* capacity envelopes on the *V-H*, *V-M*, and *H-M* planes. The *V-H* envelope corresponds to the *V-H* interaction for $M = 0$, which indicates that the largest capacity in *V-H* domain occurs at $M = 0$. However, it is interesting to note that the largest capacity in *V-M* domain does not occur at $H = 0$. Accordingly, two envelopes have been shown in the *V-M* plane. The smaller envelope corresponds to $H = 0$, whereas the larger one corresponds to a particular H (> 0) resulting in the largest capacity in *V-M* domain. The different envelopes shown in the *H-M* plane correspond to the different values of the vertrical load, *V*. It is also interesting that not only the shape and size of the *H-M* envelopes change with *V*, but also the *H-M* envlopes shift in location with varying *V*.

Another interseting observation from the *V-H-M* capacity envelopes is that a much higher vertical load can be resisted by the foundation on slope, when combined with appropriate values of positive (towards the slope) horizontal force and moment. Further, not one but two values of positive shear force, yield the same vertical load and moment capacity. It is evident from Figs. 8(a-b) and 9(a-b) that the capacity envelopes on flat ground, are not much influenced by the variation in α_h. On the other hand, in case of foundations on slopes, the capacity envelopes gradually reduced in size with increasing α_h, as can be observed from Figs. 8(c-f) and 9(c-f). Further, it can also be observed that the maximum vertical load capacity, V_{max} (with $H = M = 0$) reduced by around 35-45% and 80-90%, respectively, for the stiff clay (20°) and dense sand (30°) slopes. The reductions in maximum moment and shear capacity in negative direction are around 25-35% and 30-40%, respectively for the 20° (stiff clay) slope. In case of the 30° (dense sand) slope, even larger reductions of around 75-85% and 75-90%, respectively have been observed in the maximum moment and shear capacity in negative direction. Similarly, the reductions in maximum moment capacity in positive direction are around 15-25% and 60-75%, respectively, for stiff clay and dense sand slopes. It is interesting to note that, contrary to all other capacity parameters, the maximum shear capacity in positive

direction increases by up to 100% and 200%, respectively, for the stiff clay and the dense sand slopes, in comparison with the corresponding flat ground cases. It is to be noted here that these changes in capacity, do not represent the effect of soil type or slope inclination alone, but the combinations of slope and material properties.

Effect of vertical load on H-M seismic capacity

Figure 10 illustrtaes the effect of varying *V*, on *H-M* capacity envelopes, for strip foundation placed on surface of flat ground of stiff clay, and on top and face of the slope of the same material. The vertical load corresponding to the different *H-M* capacity envelopes in the figure is expressed as fractions of the maximum vertical load capacity, V_{max} (with $H = M = 0$) for the given slope and seismic coefficient. The capacity envelopes are shown for two values of α_h = 0 (static), and 0.2g. Figure 11 show the corresponding capacity envelopes for the flat ground consisting of dense sand material, and on top and face of the dense sand slope, for the two values of α_h. Similar capacity envelopes were obtained for other values of α_h, but are not shown here for brevity. It can be observed from the figures that, *H-M* capacity envelopes change the shape and also shift in the *H-M* plane with increasing vertical load. The shift in the envelopes indicate the asymmetry of the *V-H-M* curve in the positive and negative directions of *H* and *M*. This variation in shape and shift of the *H-M* capacity envelope defies use of a single expression (as used in (Taiebat and Carter 2000) and (Taiebat and Carter 2010) for cohessive soil and (Gottardi and Butterfield 1993) for cohessionless soil) to describe the envelope at different values of vertical load. It is interesting to note that, in all the cases, the maximum horizontal load capacity (at $M = 0$) of the foundation in the critical (negative) direction, is achieved at the vertical load ranging between one-third to half of the maximum vertical load capacity, V_{max}, whereas the maximum moment capacity is achieved at the vertical load ranging between half to two-third of V_{max}.

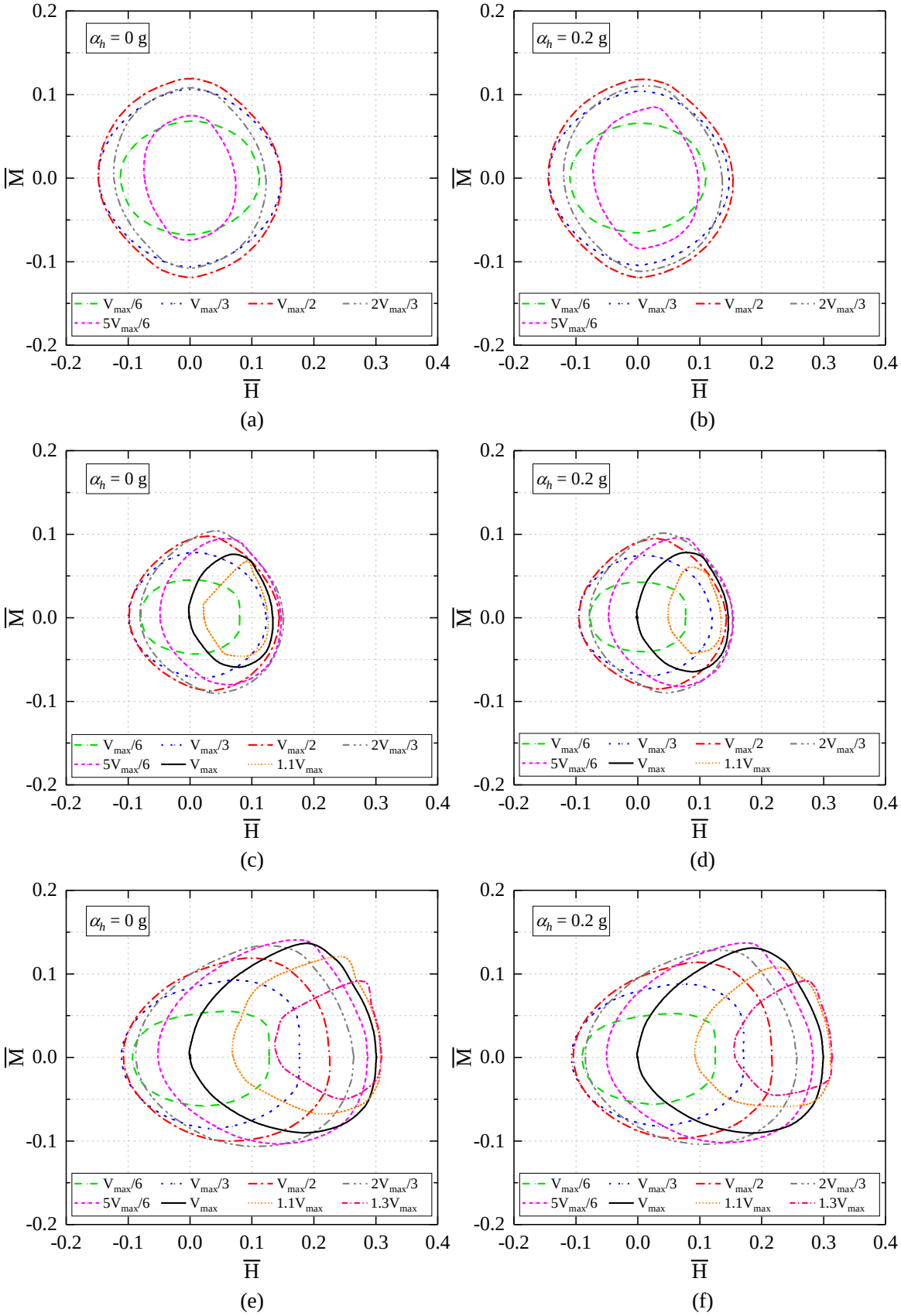

Fig. 10. *V-H-M* capacity envelopes at different V for strip foundations located on: (a) flat ground having stiff clay properties and α_h = 0 g; (b) flat ground having stiff clay properties and α_h = 0.2 g; (c) top of slope and α_h = 0 g; (d) top of slope and α_h = 0.2 g; (e) (d) face of slope and α_h = 0 g; and (f) face of slope and α_h = 0.2 g.

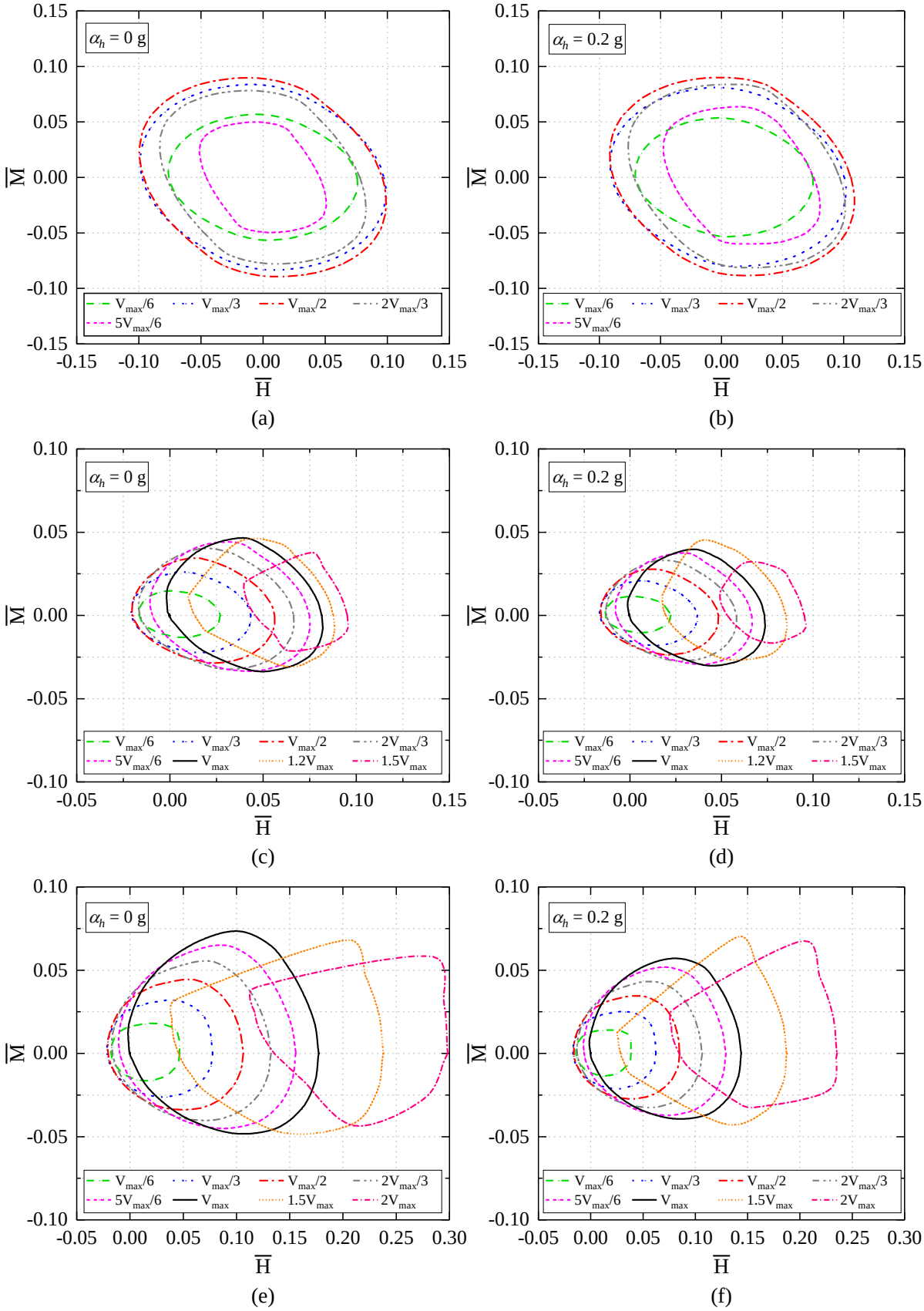

Fig. 11. *V-H-M* capacity envelopes at different V for strip foundations located on: (a) flat ground having dense sand properties and α_h = 0 g; (b) flat ground having dense sand properties and α_h = 0.2 g; (c) top of slope and α_h = 0 g; (d) top of slope and α_h = 0.2 g; (e) face of slope and α_h = 0 g; and (f) face of slope and α_h = 0.2 g.

Failure patterns

The asymmetrical effect of slope on the *V-H-M* capacity envelope can be explored by examining the failure patterns in different cases. Figure 12 shows the failure patterns (shown by contour plots of shear mobilization) for strip foundation placed on surface of flat ground of stiff clay subjected to seismic loading, α_h = 0.2g and for different combinations of *H* and *M* at a constant vertical load equal to $V_{max}/3$. Figures 13 and 14 show the failure patterns for strip foundation located on face of the stiff clay and dense sand slopes, respectively, subjected to seismic loading, α_h = 0.2g and vertical load equal to the correspondig $V_{max}/3$.

The classical two-sided failure, characterized by formation of an elastic triangular wedge below the full width of the foundation, takes place only when the foundation is on flat ground and subjected to pure vertical load approaching V_{max}. When the foundation is subjected to a combination of vertical load and moment and no horizontal load, the failure is still characterized by development of a two-sided mechanism, but the triangular elastic wedge is not formed. For all other combinations of *V*, *H* and *M*, the failure is goverened by development of one-sided mechanisms, except at very low values of *H* in combination with high values of *M*. This pattern of failure mechanisms has been found for all values of vertical load.

On the other hand, for all cases of the foundation on slope, the failure pattern is goverened by development of one-sided mechanism with shear wedge forming either in uphill or in downhill direction, though the shape of the failure surface changes for different combinations of *H* and *M*. For the combinations of positive shear and positive moment, triangular shear wedge is formed above the foundation in uphill direction, whereas under the combined action of positive shear and negative moment, a circular shear wedge is formed around the foundation resulting in failure in uphill direction. The resultant uphill failure in both these cases yields relatively higher capacity of the foundation.

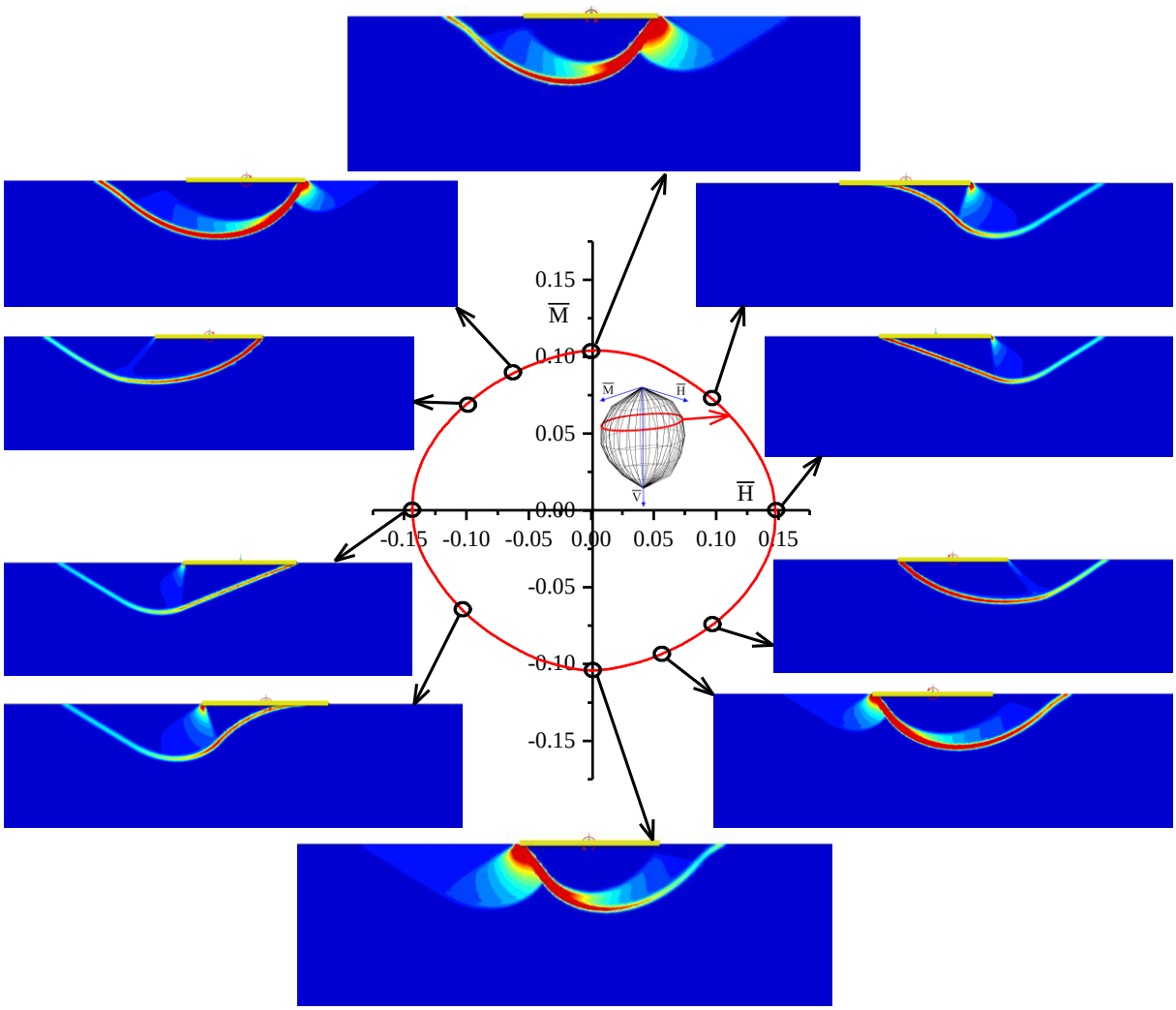

Fig. 12. Failure patterns of foundation on flat ground having stiff clay properties, under interactive *V-H-M* loads (for $V = V_{max}/3$ and $\alpha_h = 0.2$g).

Under the combined action of negative shear and negative moment, failure is caused in downhill direction and a triangular elastic wedge forms beneath the foundation. The size of triangular wedge increases gradually with increasing *H* and decreasing *M*, in the *V-H-M* combination. For the combination of negative shear and positive moment, circular or logarithmic shaped failure surface is formed in the downhill direction, without any triangular wedge beneath the foundation. The downhill side failure of the foundation yields relatively lower capacity, resulting in asymmetric shape of *V-H-M* capacity envelope.

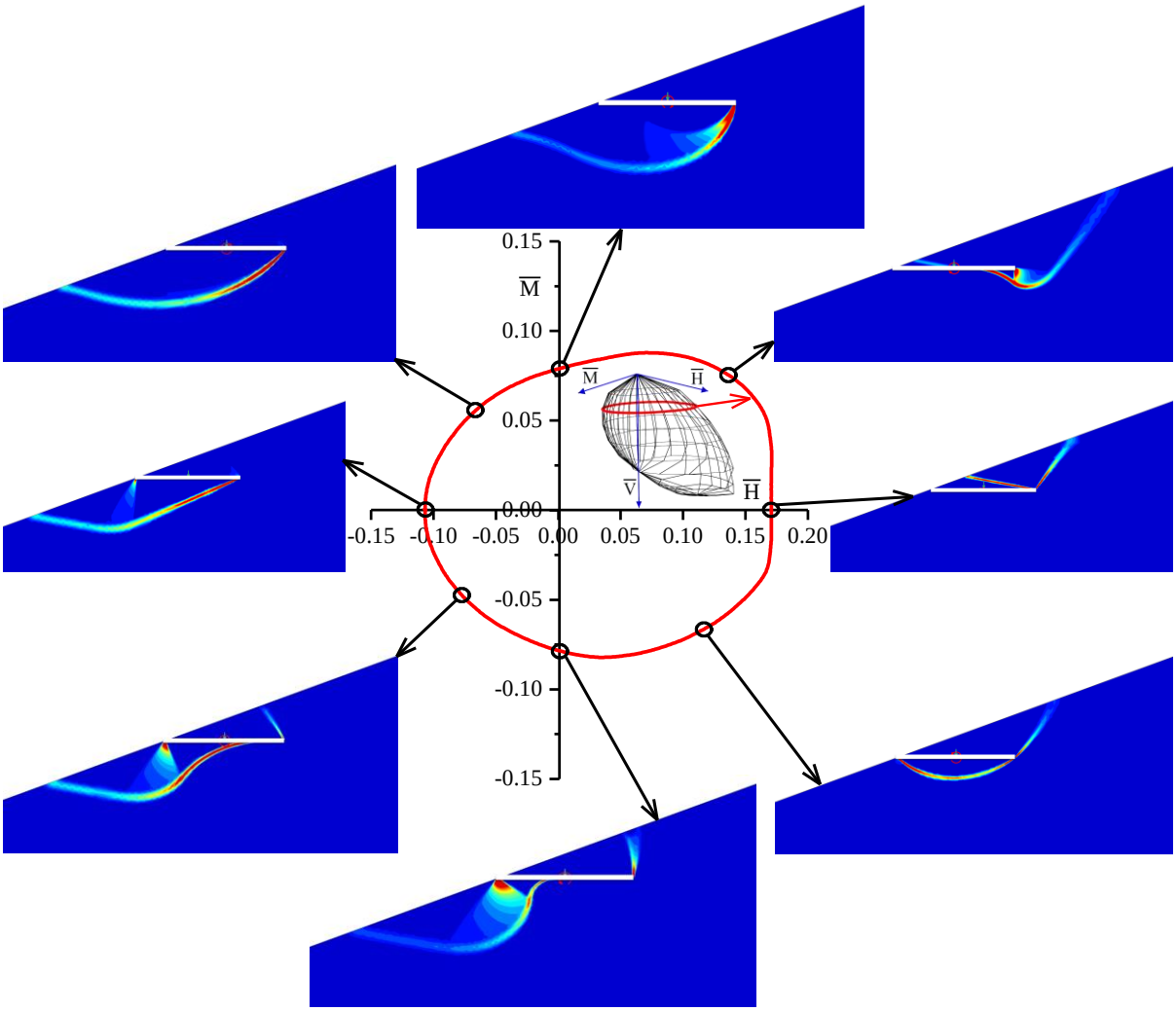

Fig. 13. Failure patterns of foundation on face of stiff clay slope, under interactive *V-H-M* loads (for $V = V_{max}/3$ and $\alpha_h = 0.2g$).

The failure mechanism in the uphill direction explains the possibility of the vertical load capacity under a particular combination of *V-H-M* being higher than that under the pure vertical load. The two directions of possible failure explain the two values of positive shear force for a given combination of moment and vertical load being higher than V_{max}. The lower value of the positive shear force corresponds the failure in downhill direction, whereas for the higher value of the positive shear force, the failure occurs in uphill direction.

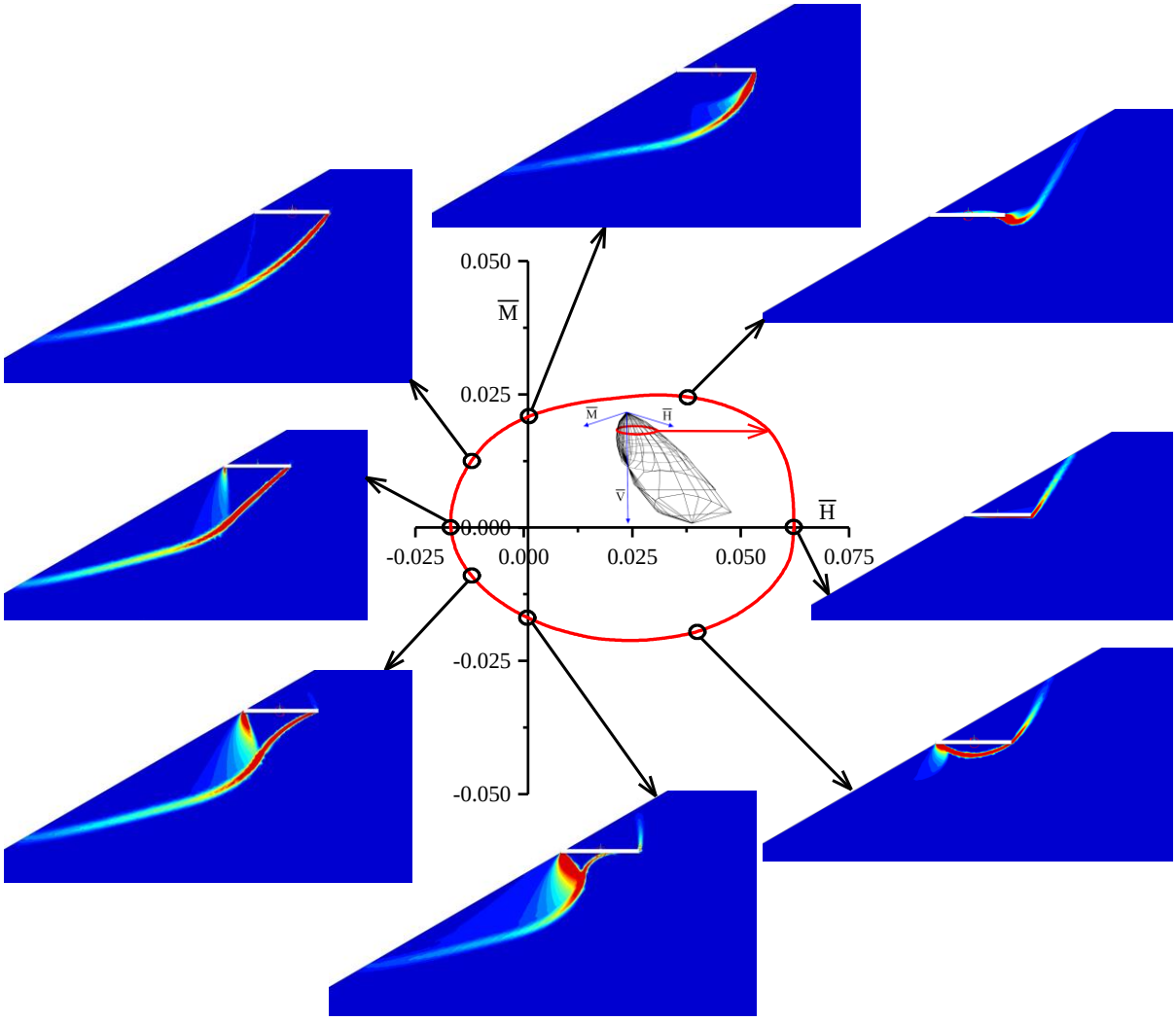

Fig. 14. Failure patterns of foundation on face of dense sand slope, under interactive *V-H-M* loads (for $V = V_{max}/3$ and $\alpha_h = 0.2g$).

Examining the hierarchy of foundation and column capacities

Almost all modern seismic design codes incorporate the concept of capacity design, in which the structural components are proportioned to yield in a particular (desired) sequence. This is achieved through a hierarchy of strength of individual components in the order of 1) foundation, 2) columns, 3) beams and 4) walls. In a conventional design, the foundations are assumed to be stiffer and stronger than the columns, so that the foundations do not yield prior to the columns. In this section, the capacity envelopes of the columns of a typical RC frame building located on a slope are compared with the capacity envelopes of the corresponding strip foundations to examine the hierarchy of the strength. A step-back configuration of a two

storey building, (the number of storeys are counted above the top-most foundation level) has been considered in this study to be located on the face of the stiff clay slope. Figure 15 shows the plan and elevation of the RC frame building considered in this study. The building has been first designed by developing a 3D fixed-base frame model in SAP2000 (2018) software, and using the relevant design codes (IS456 2000; IS1893 2016; IS13920 2016) for a Zone Factor of 0.24 g (consistent with α_h = 0.06g for the slope soil mass). A 'response reduction factor' (or behaviour factor) equal to 5 has been used in the design which takes into account the effect of yielding and inelastic energy dissipation in the supers-structure indirectly.

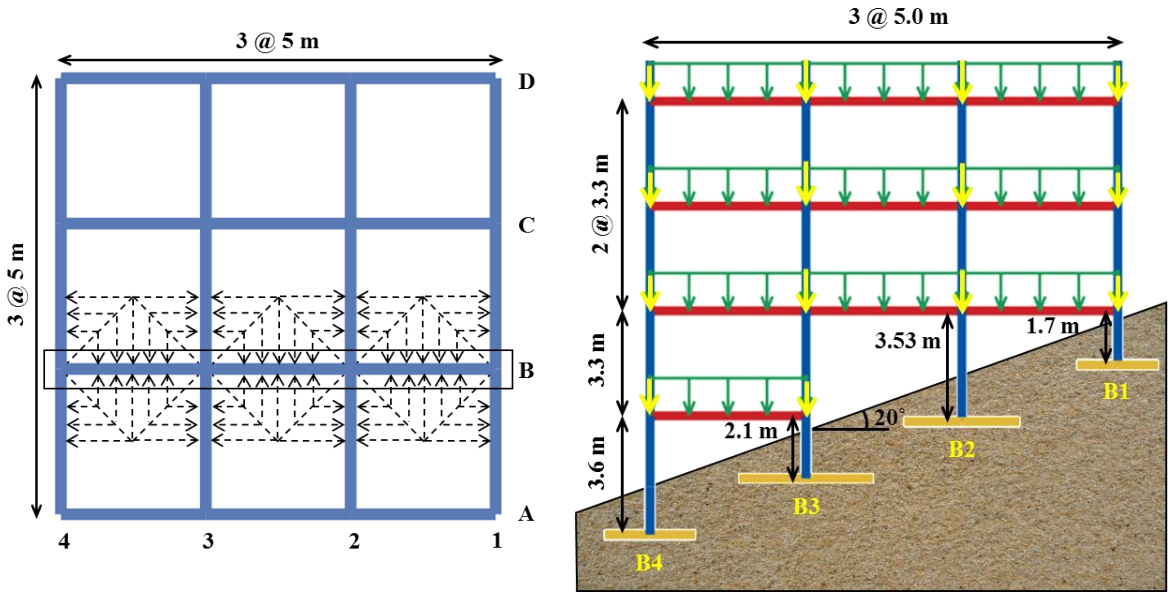

(a) (b)

Fig. 15. Plan and elevation of the considered building on stiff clay slope: (a) plan showing tributary load on a typical frame 'B'; and (b) elevation of the typical frame.

The beams and columns have been assigned the properties of M30 grade concrete (unit weight, γ = 25 kN/m^3; Poisson's ratio, ν = 0.20; Young's modulus, E = 27 GPa, and nominal cube compressive strength = 30 MPa) and Fe500 grade steel (unit weight, γ = 78.5 kN/m^3; Poisson's ratio, ν = 0.30; Young's modulus, E = 200 GPa, and nominal yield strength, f_y = 500 MPa). The beam size equal to 0.23 m × 0.40 m and the column size equal to 0.40 m × 0.40 m have been estimated following relevant design codes for reinforced concrete frame buildings

(IS456 2000; IS1893 2016; IS13920 2016). The reinforcement quantity and detailing have also been obtained using the relevant codes, but not shown here for brevity.

The foundations of the building have been designed using the design standards, e.g. (IS6403 2002; EN1997-1 2004) and literature Raj et al. (2018b), as strip foundations embedded to an average depth of 1.5 m below the soil surface. All foundations have been designed with a factor of safety equal to 3. The current standards (IS6403 2002; EN1997-1 2004) provide guidelines for estimating the static bearing capacity of foundations located on flat ground, whereas Raj et al. (2018b) have provided design aids for considering the effect of slope angle and seismic load on bearing capacity of foundation. However, this method also does not consider the *V-H-M* interaction. It is noted that EN1998-5 (2004), Annexure-F considers the effect of earthquake action in estimating bearing capacity, but it could not be used in the present case, because it does not provide capacity envelopes for foundations on c-ϕ soils.

Two representative columns B1 and B4 (Fig. 15) and corresponding foundations have been chosen for further discussion. Column B1 being the shortest column of the first storey attracts the maximum horizontal shear force but the lowest vertical force. On the other hand, the longest column B4 of the ground storey is subjected to much lower shear force and large vertical force. The foundation widths for the column B1 have been estimated as 2.4 m, 3.0 m, and 4.6 m, respectively using standards IS6403 (2002), EN1997-1 (2004) and Raj et al. (2018b). Similarly, the foundation widths for the column B4 have been estimated as 1.2 m, 1.6 m, and 2.2 m, respectively using same references.

Figure 16 shows the comparison of capacity envelopes of foundation B1 and B4 with the capacity of the respective columns, in the *V-H-M* space. The capacity envelopes of the RC columns have been developed using the material properties, size and reinforcement, obtained in design. Mander's model for confined concrete (Mander et al. 1988) and elasto-plastic constitutive model for steel has been used. The ASCE/SEI41-17 (2017) methodology

considering expected material strength and unit material partial factors of safety has been used to take into account the inherent overstrength in the conventional design of RC members. The figure also shows the projections of the *V-H-M* capacity envelopes in the *V-H*, *V-M*, and *H-M* planes. The *V-H* and *V-M* projections have been shown corresponding to *M* and *H*, respectively, equal to zero, whereas the *H-M* projections have been shown corresponding to the axial forces equal to 490 kN/m and 840 kN/m, in columns B1 and B4, respectively. The axial forces in columns have been estimated using a static analysis for gravity loads and a mode superposition analysis for seismic loads. The *V-H-M* envelope has been shown only for the foundation designed using Raj et al. (2018b), for a better visibility, whereas the planar projections (*V-H*, *V-M*, and *H-M*) have been shown for all the cases. The capacity design for the RC columns has been performed to ensure that the columns do not fail in brittle shear mode and the capacity is governed by flexure only. Further, as per the current state of the art, shear-flexure interaction is not considered to be significant in capacity estimation of RC components, and as explained earlier in Fig. 1, the moment and shear force in the columns are inter-related with a constant ratio dependent on the effective height, *h*. Therefore, the capacity envelope of the column in *H-M* plane (for a given value of *V*) collapses into two points (corresponding to the positive and negative directions of loading) indicated by the red dots in the Fig. 16.

A comparison of the capacity envelops of the columns and corresponding foundations (Fig. 16) indicates that the considered RC columns have capacities higher than those of the foundation in pure compression or tension. However, this information is not much useful as the columns during earthquake are not subjected to pure axial load. The bending moment and shear force in the columns are subjected to much larger variations during earthquake as compared to the axial load. Therefore, a more meaningful comparison can be made using *H-M* envelopes corresponding to the column axial load prevailing under gravity and earthquake actions.

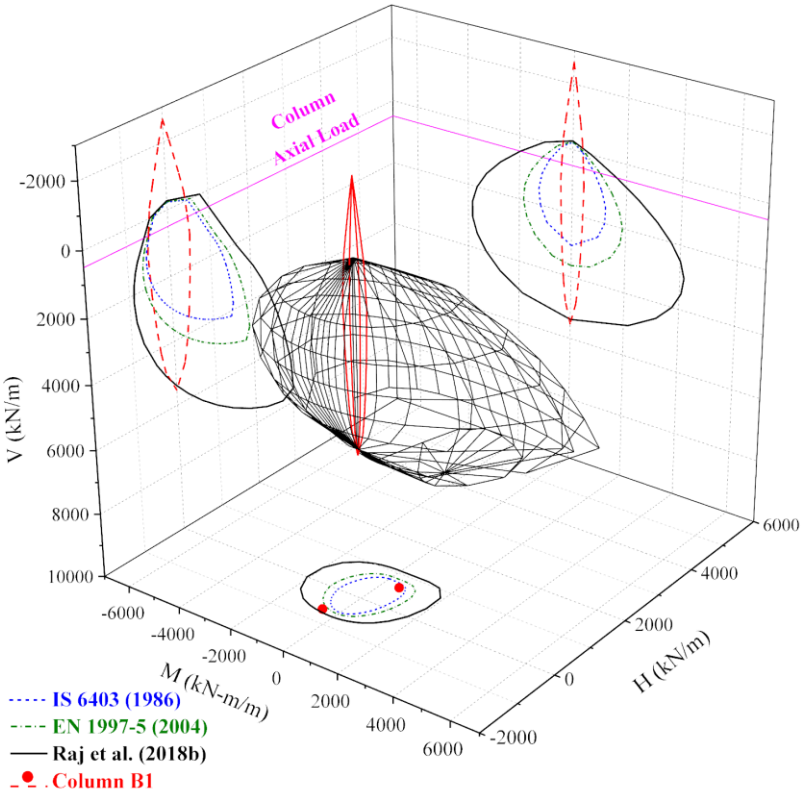

(a)

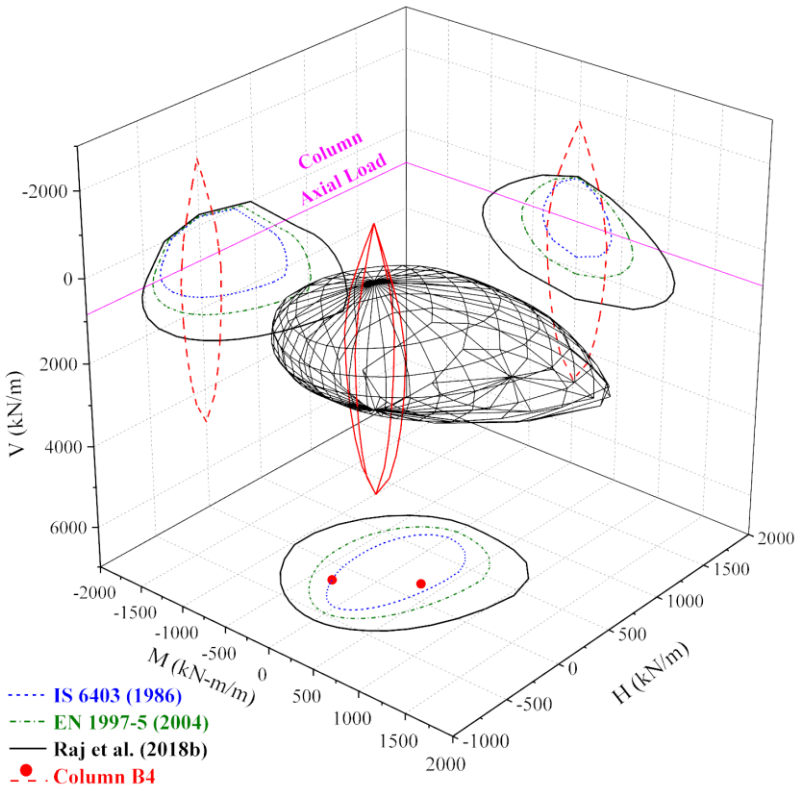

(b)

Fig. 16. Comparison of the capacity envelopes of columns with the corresponding foundations: (a) Column B1; and (b) Column B4. The two red dots in the *H-M* plane represent the capacity surface of the column. The multiple curves in *H-M* plane represent various designs of the foundations.

It can be observed from Fig. 16 that the capacity of column B1 is higher than the capacity of the foundation designed using current standards and lower than that designed using Raj et al. (2018b). On the other hand, capacity of column B4 is lower than the capacity of the foundation B4 designed using all the methods. It is to be noted that in case of buildings on slopes, not only the effect of earthquake action is different on the soil and the superstructure, it varies significantly from column to column due to their unequal heights. These results highlight the need to consider the capacity envelope method for design of foundations, located on slopes especially in seismic areas.

Conclusions

A numerical study has been performed to understand the behaviour and failure modes of strip foundations placed at different locations on stable slopes, subjected to seismic loading. The behaviour and capacity envelopes of strip foundations placed on slopes and subjected to general planar (*V-H-M*) loading, have been compared with their counterpart soil-foundation systems on flat ground. It has been observed that the classical failure mechanism consisting of symmetric shear failure and elastic triangular wedge utilizing full foundation width takes place only in case of foundations located on flat ground and subjected to pure vertical load applied at the centre of the foundation. Even in case of foundations located on flat ground, asymmetric/one-sided failure mechanism is observed, when subjected to a combination of horizontal shear and/or moment with the vertical load.

In case of foundations located on slopes, the failure pattern consists of one sided shear wedge forming either in uphill or in downhill direction, though the shape of the failure surface changes for different combinations of *H* and *M*. The shear wedge forming in uphill direction results in relatively higher capacity than the downhill direction. Further, the failure mechanism in the uphill direction also explains the possibility of the vertical load capacity (under a

particular combination of *V-H-M*) being higher than that under the pure vertical load. The two directions, uphill and downhill, of possible failure, explain the two values of positive shear force, for a given combination of moment and vertical load, higher than V_{max}. The lower value of the positive shear force corresponds the failure in downhill direction, whereas the higher value of the positive shear force, the failure occurs in uphill direction.

The capacity envelopes of foundations on slopes, reveal that the *V-H-M* capacity envelope is asymmetric for positive and negative directions of *H* and *M*. The largest capacity in *V-H* domain occurs at $M = 0$, but, the maximum capacity in *V-M* domain does not occur at $H = 0$. It is interesting to note that not only the shape and size of the *H-M* envelopes changes with varying *V*, the *H-M* envlopes shift their location with varying *V*. Further, it has been noted that the maximum horizontal load capacity (at $M = 0$), of the foundation, in the critical (negative) direction, is achieved for the vertical load ranging from $V_{max}/3$ to $V_{max}/2$, whereas the maximum moment capacity is achieved at the vertical load ranging from $V_{max}/2$ to $2V_{max}/3$.

The capacity envelopes for foundations on flat ground, are not much influenced by the variation in α_h, whereas in case of foundations on slopes, the capacity envelopes become gradually reduced subsets of the respective static case ($\alpha_h = 0$) with increase in α_h. The maximum vertical load capacity, V_{max} (with $H = M = 0$) reduced significantly for the dense sand (30°) slope compared to stiff clay (20°) slope. A significant reduction (ranging between 25% and 90%) in the maximum moment and shear capacity (in comparison with the same foundations on flat ground) in negative direction has been observed for the both 20° (stiff clay) and 30° (dense sand) slopes, subjected to α_h varying from 0 to 0.3g. The reduction in maximum moment capacity in positive direction has been comparatively lesser than the negative direction for both the slopes. The reduction was more prominent in case of 30° (dense sand) slope. Contrary to all other capacity parameters, the maximum shear capacity in positive direction increases up to 2 and 3 times, respectively, for the stiff clay and the dense sand slopes.

A comparison of the capacity enevelopes of the typical foundations on slope with the corresponding columns, reveals that the current design methods may be non-conservative or highly conservative, in different cases, as these methods do not take into consideration the interactive *V-H-M* actions transmitted by the columns to the foundations. To ensure the desired failure mechanism in capacity design framework, it is important to design the foundations using *V-H-M* capacity envelope, especially in case of foundations located on slopes in seismic areas.

Acknowledgments

The research work presented here was supported by the Institute fellowship to the first author from the Ministry of Human Resource Development, Government of India. The authors are grateful to 'Optum Computational Engineering' (OptumCE) for providing free academic license of OptumG2 software to perform the present study.

References

ASCE/SEI41-17 (2017) Seismic Evaluation and Retrofit of Existing Buildings. American Society of Civil Engineers, Reston, Virginia. doi:10.1061/9780784414859

Baazouzi M, Benmeddour D, Mabrouki A, Mellas M (2016) 2D Numerical Analysis of Shallow Foundation Rested Near Slope under Inclined Loading. Procedia Engineering 143:623-634 doi:10.1016/j.proeng.2016.06.086

Bransby MF, Randolph MF (1998) Combined loading of skirted foundations. Géotechnique 48:637-655 doi:10.1680/geot.1998.48.5.637

Butterfield R, Gottardi G (1994) A complete three-dimensional failure envelope for shallow footings on sand. Géotechnique 44:181-184 doi:10.1680/geot.1994.44.1.181

Butterfield R, Houlsby GT, Gottardi G (1997) Standardized sign conventions and notation for generally loaded foundations. Géotechnique 47:1051-1054 doi:10.1680/geot.1997.47.5.1051

Chen WF, Liu XL (1990) Limit analysis in soil mechanics. Elsevier, Amsterdam

Cocjin M, Kusakabe O (2013) Centrifuge observations on combined loading of a strip footing on dense sand. Géotechnique 63:427-433 doi:10.1680/geot.11.P.075

EN1997-1 (2004) Eurocode 7: Geotechnical design - Part 1: General rules. British Standards Institution, London

EN1998-5 (2004) Eurocode 8: Design of Structures for Earthquake Resistance - Part 5: Foundations, retaining structures and geotechnical aspects, Sixth Revision edn. British Standards Institution, London

Fotopoulou SD, Pitilakis KD (2013) Fragility curves for reinforced concrete buildings to seismically triggered slow-moving slides. Soil Dynamics and Earthquake Engineering 48:143-161 doi:10.1016/j.soildyn.2013.01.004

Georgiadis K (2010) The influence of load inclination on the undrained bearing capacity of strip footings on slopes. Computers and Geotechnics 37:311-322 doi:10.1016/j.compgeo.2009.11.004

Gottardi G, Butterfield R (1993) On the bearing capacity of surface footings on sand under general planar loads. Soils and Foundations 33:68-79 doi:10.3208/sandf1972.33.3_68

Gottardi G, Butterfield R (1995) The displacement of a model rigid surface footing on dense sand under general planar loading. Soils and Foundations 35:71-82 doi:10.3208/sandf.35.71

Gottardi G, Houlsby GT, Butterfield R (1999) Plastic response of circular footings on sand under general planar loading. Géotechnique 49:453-469 doi:10.1680/geot.1999.49.4.453

Gourvenec S (2007a) Shape effects on the capacity of rectangular footings under general loading. Géotechnique 57:637-646 doi:10.1680/geot.2007.57.8.637

Gourvenec S (2007b) Failure envelopes for offshore shallow foundations under general loading. Géotechnique 57:715-728 doi:10.1680/geot.2007.57.9.715

Gourvenec S (2008) Effect of embedment on the undrained capacity of shallow foundations under general loading. Géotechnique 58:177-185 doi:10.1680/geot.2008.58.3.177

Gourvenec S, Randolph M (2003) Effect of strength non-homogeneity on the shape of failure envelopes for combined loading of strip and circular foundations on clay. Géotechnique 53:575-586 doi:10.1680/geot.2003.53.6.575

Govoni L, Gourvenec S, Gottardi G (2010) Centrifuge modelling of circular shallow foundations on sand. International Journal of Physical Modelling in Geotechnics 10:35-46 doi:10.1680/ijpmg.2010.10.2.35

IS456 (2000) Plain and Reinforced Concrete - Code of Practice. Bureau of Indian Standard, New Delhi

IS1893 (2016) Crieteria for Eathquake Resistance Design of Structures, Part 1 General Provisons and Buildings. Bureau of Indian Standard, New Delhi

IS6403 (2002) Code of Practice for Determination of Bearing Capacity of Shallow Foundations. Bureau of Indian Standards, New Delhi

IS13920 (2016) Ductile Detailing of Reinforced Concrete Structures Subjected to Seismic Forces - Code of Practice, Sixth Revision edn., Bureau of Indian Standard, New Delhi

Krabbenhoft K, Lyamin A, Krabbenhoft J (2016) OptumG2: Theory. Optum Computational Engineering, Available on: https://optumce.com/wp-content/uploads/2016/05/Theory.pdf

Lesny K (2006) The role of favourable and unfavourable actions in the design of shallow foundations according to Eurocode 7. In: Parsons RL, Zhang L, Guo WD, Phoon KK,

Yang M (eds) Foundation Analysis and Design : Innovative Methods, vol GSP-153. American Society of Civil Engineers. doi:10.1061/40865(197)15

Lesny K (2009) Safety of shallow foundations – Limit State Design according to Eurocode 7 vs. alternative design concepts. Georisk: Assessment and Management of Risk for Engineered Systems and Geohazards 3:97-105 doi:10.1080/17499510802552877

Loukidis D, Chakraborty T, Salgado R (2008) Bearing capacity of strip footings on purely frictional soil under eccentric and inclined loads. Canadian Geotechnical Journal 45:768-787 doi:10.1139/T08-015

Makrodimopoulos A, Martin CM (2006) Lower bound limit analysis of cohesive-frictional materials using second-order cone programming. International Journal for Numerical Methods in Engineering 66:604-634 doi:10.1002/nme.1567

Makrodimopoulos A, Martin CM (2007) Upper bound limit analysis using simplex strain elements and second-order cone programming. International Journal for Numerical and Analytical Methods in Geomechanics 31:835-865 doi:10.1002/nag.567

Mander JB, Priestley MJN, Park R (1988) Theoretical stress-strain model for confined concrete. Journal of Structural Engineering 114:1804-1826 doi:10.1061/(ASCE)0733-9445(1988)114:8(1804)

Martin CM, Houlsby GT (2000) Combined loading of spudcan foundations on clay: laboratory tests. Géotechnique 50:325-338 doi:10.1680/geot.2000.50.4.325

Montrasioa L, Nova R (1997) Settlements of shallow foundations on sand: Geometrical effects. Géotechnique 47:49-60 doi:10.1680/geot.1997.47.1.49

NCHRP (2010) Report 651: LRFD Design and Construction of Shallow Foundations for Highway Bridge Structures. National Cooperative Highway Research Program, Transportation Research Board, Washington, D.C. doi:10.17226/14381

Nova R, Montrasioa L (1991) Settlements of shallow foundations on sand. Géotechnique 41:243-256 doi:10.1680/geot.1991.41.2.243

OptumG2 (2018) v2.2018.02.09, Optum Computational Engineering. Copenhagen NV, Denmark

Raj D, Singh Y, Kaynia AM (2018a) Behavior of slopes under multiple adjacent footings and buildings. International Journal of Geomechanics 18 doi:10.1061/(ASCE)GM.1943-5622.0001142

Raj D, Singh Y, Shukla SK (2018b) Seismic bearing capacity of strip foundation embedded in c-ϕ soil slope. International Journal of Geomechanics 18 doi:10.1061/(ASCE)GM.1943-5622.0001194

SAP2000 (2018) v20, Computers and Structures Inc., Berkeley.

Shen Z, Feng X, Gourvenec S (2016) Undrained capacity of surface foundations with zero-tension interface under planar V-H-M loading. Computers and Geotechnics 73:47-57 doi:10.1016/j.compgeo.2015.11.024

Sloan SW (2013) Geotechnical stability analysis. Géotechnique 63:531-572 doi:10.1680/geot.12.RL.001

Taiebat HA, Carter JP (2000) Numerical studies of the bearing capacity of shallow foundations on cohesive soil subjected to combined loading. Géotechnique 50:409-418 doi:10.1680/geot.2000.50.4.409

Taiebat HA, Carter JP (2010) A failure surface for circular footings on cohesive soils. Géotechnique 60:265-273 doi:10.1680/geot.7.00062

Tang C, Phoon K-K, Toh K-C (2015) Effect of footing width on Nγ and failure envelope of eccentrically and obliquely loaded strip footings on sand. Canadian Geotechnical Journal 52:694-707 doi:10.1139/cgj-2013-0378

Ukritchon B, Whittle AJ, Sloan SW (1998) Undrained limit analyses for combined loading of strip footings on clay. Journal of Geotechnical and Geoenvironmental Engineering 124:265-276 doi:10.1061/(ASCE)1090-0241(1998)124:3(265)

Vulpe C, Gourvenec S, Power M (2014) A generalised failure envelope for undrained capacity of circular shallow foundations under general loading. Géotechnique Letters 4:187-196 doi:10.1680/geolett.14.00010

Yun G, Bransby MF (2007) The horizontal-moment capacity of embedded foundations in undrained soil. Canadian Geotechnical Journal 44:409-424 doi:10.1139/t06-126